Squeezed film damping measurements on a parallel-plate MEMS in the free molecule regime

2009 J. Micromech. Microeng. 19 074021

(http://iopscience.iop.org/0960-1317/19/7/074021)

J. Micromech. Microeng. **19** (2009) 074021 (6pp) doi:10.1088/0960-1317/19/7/074021

Squeezed film damping measurements on a parallel-plate MEMS in the free molecule regime

L Mol[1], L A Rocha[2], E Cretu[3] and R F Wolffenbuttel[1]

[1] Department MicroElectronis/EI, Faculty EEMCS, Delft University of Technology, Mekelweg 4, 2828 CD Delft, The Netherlands
[2] Department of Industrial Electronics, University of Minho, Campus de Azurém, 4800-058 Guimarães, Portugal
[3] Department of Electrical and Computer Engineering, University of British Columbia, 2332 Main Mall, Vancouver, BC V6T 1Z4, Canada

E-mail: l.mol@tudelft.nl

Received 19 December 2008, in final form 27 April 2009
Published 30 June 2009
Online at stacks.iop.org/JMM/19/074021

Abstract
This paper provides experimental validation of the predictions by two recent models for squeezed film damping in the free molecule regime. Measurements were carried out using a parallel-plate microstructure with a 2.29 μm gap operated at pressures from 10^5 to 10^1 Pa (corresponding to Knudsen numbers from 0.03 to 300). Experiments are in good agreement with the modelling based on molecular dynamics at Knudsen numbers over 10. The result also indicates that modelling based on the modified Reynolds equation including inertia effects underestimates the damping due to end effects; however, it correctly predicts the trend for lower Knudsen numbers.

(Some figures in this article are in colour only in the electronic version)

1. Introduction

Accurate modelling of squeezed film damping of rarefied gas in MEMS structures is of crucial importance for a reliable prediction of their dynamic performance. Examples of MEMS applications where the effect of gas damping is an important factor in the operating characteristics include RF switches, resonators, accelerometers, gyroscopes and micro-mirrors. The damping effect, for example, determines the quality factor of resonators and the switch speed of RF switches.

For structures with sufficiently large dimensions or those operated at—or just slightly below—ambient pressure, continuum-mechanics-based models can be used to predict the damping effect due to the surrounding gas [1]. However, for sub-micron-sized gaps or when operating at pressures close to vacuum, the interaction of the individual gas molecules with the structure becomes dominant over the internal viscous forces and modelling of the so-called free molecule regime is needed in order to obtain valid device performance predictions.

A recent overview of the topic of squeezed film damping in a MEMS [2] shows that current research focuses mainly on the analytical approach and the simulation tools used for the continuum regime. The rarefied gas regime modelling receives much less attention. Furthermore, experimental data in the literature suitable for verification of the models and simulation tools are scarce. This is especially true for the free molecular domain. Also the experimental data that are available are not always ideally suited for model validation, due to discrepancies in the boundary conditions between the models and the physical devices [3, 4].

With the ongoing trend towards ever-decreasing MEMS feature sizes, the importance of the accurate modelling of free molecular gas flow will only increase. Extensive validation of the proposed models is, therefore, needed. This work presents damping measurements obtained from a parallel-plate microstructure operated over a wide pressure range spanning four decades. Two of the most prominent free molecule regime damping models in the literature are examined and used to compare with the experimental results.

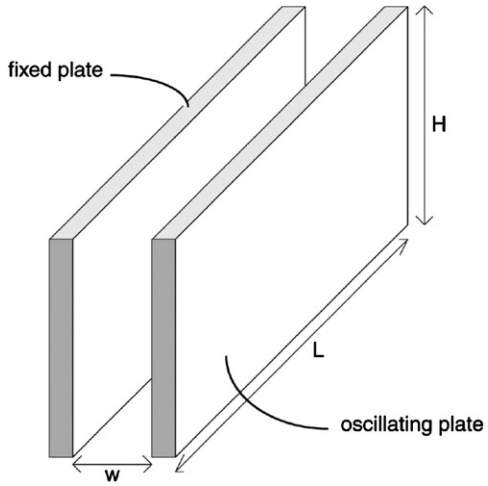

Figure 1. Two plates of length L and height H define a channel of width w. The gas in the gap between the plates causes a damping force to counteract the movement of the oscillating plate.

First, the two models for squeeze-film damping of rarefied gas are introduced in section 2. Next, section 3 will introduce the measurement methodology that is used to extract the damping ratio and damping coefficient from a second-order system response. Subsequently, in section 4 the experimental set-up is described, followed by the results in section 5. Finally, the conclusions are presented in section 6.

2. Squeezed film damping

2.1. Continuum versus free molecule regime

When a volume of gas is displaced due to motion of its confining boundaries the gas interacts with the structure surrounding it, thereby creating an energy dissipating effect. This effect manifests itself as a damping force on the moving boundary (i.e. the structure). The fundamental variable to consider is the ratio of the mean free path of a gas molecule to the typical channel width. This ratio is called the Knudsen number K_n [5]. The mean free path length λ is given as [14]

$$\lambda = \frac{RT}{\pi\sqrt{2}d^2 N_A p}, \tag{1}$$

where R is the gas constant, T is the temperature, d is the molecule diameter, p is the pressure and N_A is the Avagadro number. For gas flowing in a rectangular channel composed of two plates of a finite aspect ratio L/H (figure 1), the Knudsen number K_n thus expresses the ratio of the mean free path length λ of the gas molecules to the channel width w as $K_n = \lambda/w$. For a constant gap size w, the Knudsen number is therefore inversely proportional to the pressure.

As long as the pressure of the gas surrounding the structure is high enough, or device feature sizes are large enough, the Knudsen number is small. Consequently, the gas behaves as a viscous fluid and continuum mechanics apply. The Reynolds equation based on the Navier–Stokes equation and general viscous hydrodynamics equations can be used to model the gas flow [6, 7]. However for Knudsen numbers larger than about 10, the interaction of the individual gas molecules with the device starts to dominate over the internal viscous forces. This is called the free molecule regime. Several gas damping models for this regime have been proposed and consequently modified and enhanced by others [8–12]. Two general modelling approaches exist for the rarefied gas regime. This work uses one promising model of each type for comparison.

The first modelling approach is based on the models from the continuum regime. To accommodate the gas rarefaction, the models use a modified gas viscosity. Sumali [4] investigated such a model introduced by Veijola. Based on comparative experimental validation, he concludes that Veijola's model based on the Reynolds equation with inertia effects [13] is the most accurate.

The second modelling approach is based on the individual interactions of gas molecules with the MEMS. An interesting model of this second type by Hutcherson [14] is based on a simulation of the molecular dynamics and is also further investigated in this work.

2.2. Reynolds equation with inertia

Veijola has derived a modified Reynolds equation including gas inertia and rarefaction effects [12]:

$$\frac{\partial}{\partial x}\left(\frac{\rho h^3}{12\eta}Q_{pr}\frac{\partial p}{\partial x}\right) + \frac{\partial}{\partial y}\left(\frac{\rho h^3}{12\eta}Q_{pr}\frac{\partial p}{\partial y}\right) = \frac{\partial(\rho h)}{\partial t}, \tag{2}$$

where ρ is the density, η is the viscosity, h is the momentary position of the oscillating plate at nominal spacing w and Q_{pr} is the relative flow rate coefficient:

$$Q_{pr} = \frac{1 + 6K_n}{1 + j\omega\frac{\rho h^2\left(1 + 10K_n + 30K_n^2\right)}{10\eta(1 + 6K_n)}}. \tag{3}$$

The resulting solution for the damping coefficient b for rectangular parallel plates is expressed as

$$\begin{aligned} b_{M,N} &= \sum_{m=\text{odd}}^{M}\sum_{n=\text{odd}}^{N}\frac{1}{Q_{pr}G_{m,n} + j\omega C_{m,n}}, \\ G_{m,n} &= \frac{\pi^6 h^3 (mn)^2}{768\eta LH}\left(\frac{m^2}{L^2} + \frac{n^2}{H^2}\right) \\ C_{m,n} &= \frac{\pi^4 h (mn)^2}{64 P_a LH}, \end{aligned} \tag{4}$$

where m and n are odd integers and M and N should be chosen sufficiently large.

2.3. Molecular dynamics code

Bao developed a model based on the energy transfer between gas molecules and an oscillating micro-structure [12]. It is based on the changes in the velocity of a molecule that collides with a moving structure. According to Bao, the damping coefficient is

$$b_{Bao} = \frac{(H + L)/w}{4\pi}\sqrt{\frac{2m_m}{\pi k_B T}}\text{LHP}_a. \tag{5}$$

To obtain this closed form expression, Bao made three assumptions: constant particle velocity, constant change in

particle velocity and constant beam position. Hutcherson later showed one of these assumptions—the constant particle velocity—to be incorrect [14]. Hutcherson consequently developed a molecular dynamics (MD) simulation code that tracks the interaction of each individual molecule in the gap. It is based on the energy transfer model of Bao, however without the constraining assumptions made by Bao. The MD code is a numerical method that is computationally intensive; however, the results in [4] indicate that modelling by Bao underestimates the damping force by a factor of 2.23 as compared to Hutcherson's model.

3. Measurement method

In order to verify the validity of the existing models, damping measurements are needed. Different experimental methods exist to extract the damping coefficient from a micro-structure. Sumali uses experimental modal analysis [4], a technique operating in the frequency domain, which characterizes the transfer function of a device based on its response to a known vibration input. Its disadvantage is the need for a mechanical excitation source, which complicates a practical experimental set-up significantly.

The technique used in this work operates in the time domain and is based only on the intrinsic behaviour of the micro-structure. Following is an analysis of second-order system behaviour and the way to extract damping measurements from simple system relaxation measurements.

3.1. Second-order system behaviour

The dynamic behaviour of the inertial MEM device without external input forces is described by the second-order system equation:

$$m\ddot{z} + b\dot{z} + kz = 0, \tag{6}$$

where z denotes the displacement, m the device mass, b the damping coefficient and k the spring constant. Inserting parameters

$$\omega_n = \sqrt{\frac{k}{m}} \quad \text{and} \quad \zeta = \frac{b}{2\sqrt{\text{km}}} \tag{7}$$

enables equation (6) to be rewritten as

$$\ddot{z} + 2\zeta\omega_n\dot{z} + \omega_n^2 z = 0. \tag{8}$$

Here, ω_n is the undamped natural frequency, while ζ is the damping ratio and determines if the system is over-damped ($\zeta > 1$), critically damped ($\zeta = 1$) or under-damped ($\zeta < 1$).

In case the system is under-damped, the solution to the differential equation (8) is

$$z(t) = A\mathrm{e}^{-\zeta\omega_n t}\sin(\sqrt{1-\zeta^2}\omega_n t + \varphi). \tag{9}$$

From this expression, it is clear that a harmonic displacement signal is enveloped by an exponential decay term that depends on the damping ratio ζ and the natural frequency ω_n of the device.

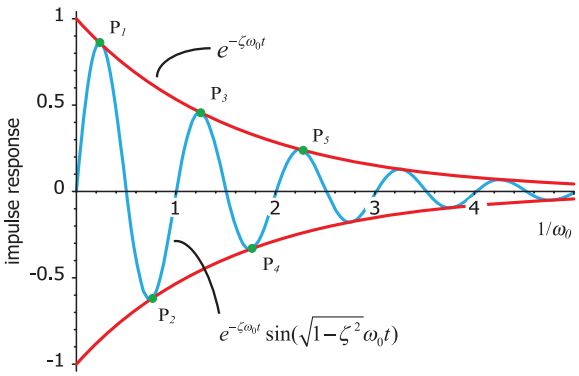

Figure 2. The impulse response of an under-damped second-order system with $\omega_n = 1$ and $\zeta = 0.1$. The first six peaks are indicated as $p[1,\ldots,6]$.

3.2. Extracting the damping ratio

Figure 2 shows a typical under-damped system impulse response; the first six peaks $p_{1,\ldots,6}$ are also indicated. The amplitude ratio of p_n to p_{n+2} is constant and equal to $p_{n+2}/p_n = \mathrm{e}^{-\zeta 2\pi}$. Hence, the value of ζ can be obtained from the rate of the decay of a measured response signal. In a practical experiment, the end value of the signal of finite duration is not necessarily zero, which makes it impossible to get absolute amplitudes of the peaks $p_{1,\ldots,n}$. This is avoided by using the difference values of two peaks, i.e. $p_1 - p_2$, $p_3 - p_2$, $p_3 - p_4$, etc. The sequence of difference values still depends on the damping ratio but is independent of any common mode signal.

The resulting sequence of peak differences is used for fitting an exponential decay function whose exponent is the rate of decay and contains the damping ratio ζ. The damping coefficient results when also considering the values of the other system parameters.

An alternative approach uses the Hilbert transform to represent the measured signal (9) as an analytical signal. As long as the rate of decay is long compared to the natural resonance period $1/\omega_\mathrm{n}$ the Hilbert transform can be used in an envelope detection method to extract the rate of decay. Since this method can only be used for highly under-damped structures, it cannot be used in this work.

4. Measurement set-up

4.1. 1-DOF MEMS device

An electro-statically actuated 1-DOF MEMS structure with separate drive and sense electrodes has been designed and fabricated in an SOI process [16] featuring a 25 μm device layer thickness (figure 3). The device consists of a central mass suspended on four folded springs. Four distinct sets of electrodes are attached to a central moving bar, which are interleaved with electrodes that are fixed to the substrate. The two narrow beam sets form a differential capacitor that is used to read out the device displacement, while each of the wider beam sets is used to excite the mass through electrostatic actuation in either direction. Table 1 lists the key properties of the device.

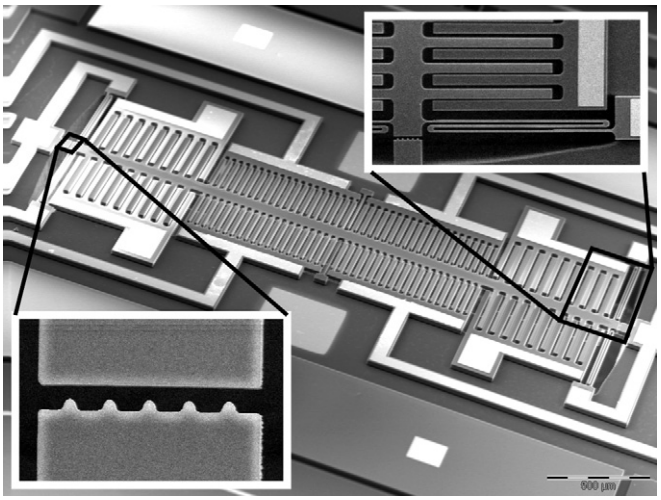

Figure 3. SEM image of the fabricated device. The narrow electrodes in the centre form the sensing capacitors and the wider ones on the outside are for electrostatic actuation. The insets show the details of a spring, a stopper and actuation electrodes.

The fabrication process includes a back side etch that removes the handling wafer directly beneath the active device area. The advantage of this approach, as compared to conventional sacrificial etching, is the elimination of any influence of neighbouring surfaces on the gas channel. The resulting gas channel therefore very closely resembles the modelled channel.

4.2. Capacitive read-out circuit

The displacement read-out is implemented with a two-channel differential charge amplifier circuit and a coherent detection mixer realized in a single custom 0.35 μm CMOS chip (figure 4). The overall displacement uncertainty of the combined set-up at a 2.8 kHz bandwidth is 1.6 nm.

Table 1. 1-DOF MEMS device properties.

Property	Value	Unit
Mass (m)	42.0	μg
Spring constant (k)	12.9	N m^{-1}
Undamped natural frequency	2.84	kHz
Sense capacity (C_s)	1.12	pF
Device layer thickness (H)	25.0	μm
Length sense arm (L_s)	230	μm
Length actuation arm (L_a)	300	μm
Number of sense arms (N_{sa})	40	
Number of actuation arms (N_{aa})	18	
Small gap size (w_0)	2.29	μm
Large gap size sense electrodes (w_{1s})	14.3	μm
Large gap size actuation electrodes (w_{1s})	12.3	μm

4.3. Measuring at varying pressures

A pcb with the MEMS device and the read-out circuit is operated in a vacuum chamber. The pressure of the gas (i.e. air) can be varied from atmospheric pressure down to 0.1 mbar. This corresponds to Knudsen numbers for the smallest gap ranging from 0.03 to 300.

The device is displaced from its initial position by applying a voltage to one of the actuation capacitors. When the voltage is removed, the device returns to its initial position and behaves like a simple second-order system without any external input forces. The measured relaxation response is sampled with a data acquisition card and Matlab is used for further signal processing. Figure 5 shows a typical measurement together with the resulting curve fit obtained from Matlab.

5. Experimental results

Using the models from section 2 with the device properties of table 1, the expected damping coefficient for various pressures is calculated according to the three models. Figure 6 presents the measurement results together with the damping according to the models. Bao's model and the estimation of Hutcherson's

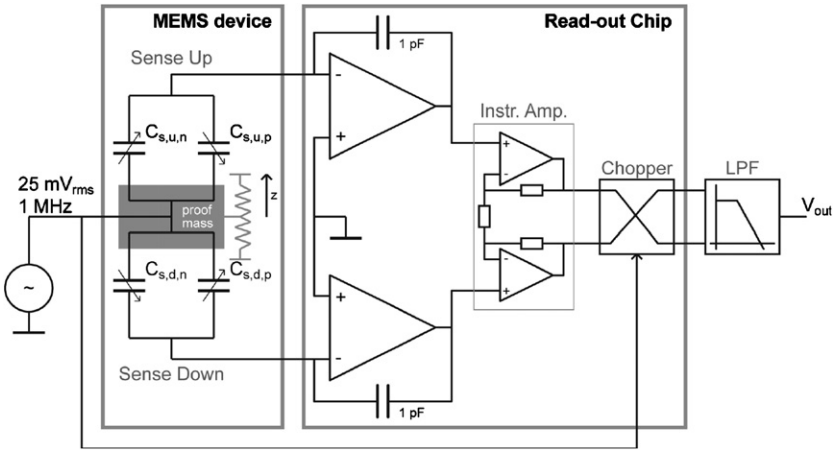

Figure 4. Simplified schematic of the total read-out circuit.

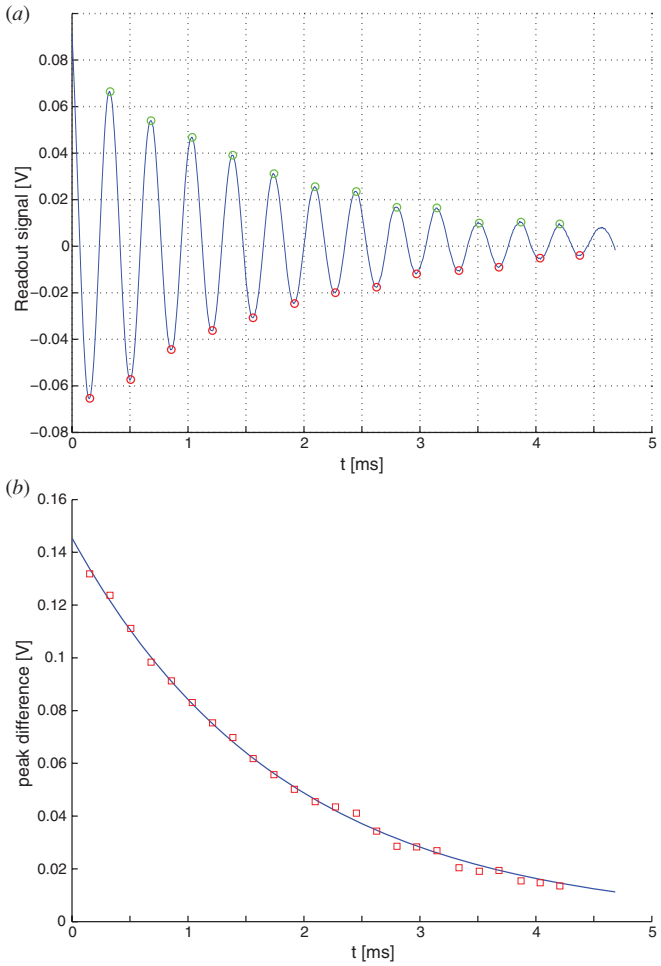

Figure 5. (*a*) Device relaxation measurement after an initial disturbance from its equilibrium position. (*b*) The resulting Matlab curve fit for the exponentially decaying envelope function.

model are only valid for the free molecular regime and indeed deviate from the trend in the measurement results present at higher pressures. Veijola's model underestimates the damping forces by more than 50%. This is most likely caused by the assumption of zero pressure difference at the channel borders. This assumption is only valid when the gap size is small compared to the plate dimensions, which is not the case in our device. The estimated Hutcherson's model fits the measured data with less than 5% error in the free molecular regime.

6. Conclusions and future work

Experimental squeeze-film gas damping data were obtained from step response measurements on a parallel-plate electrostatic microstructure within a range of pressures that covers both the viscous regime and the free molecule regime. The measurements demonstrate that the modelling based on molecular dynamics appropriately describes damping for Knudsen numbers higher than 10. Comparison with a model based on the Reynolds equation that includes gas inertia effects not only shows a significant underestimation, but also

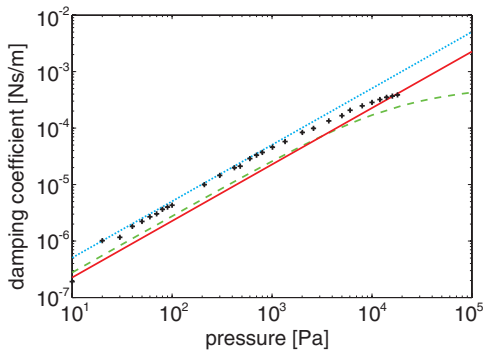

Figure 6. Measurement results (+) compared to the model of Bao (solid line), estimation of Hutcherson (dotted line) and Veijola (dashed line).

provides experimental validation of the trend at lower Knudsen numbers. This suggests that further investigation is needed to account for the end effects present in practical channels with dimensions comparable to the gap size.

Currently, we are performing additional measurements at different gap sizes and with other gas types. This is expected to further extend the usability of these measurements for validation of existing models.

Acknowledgments

Parts of this work would not have been possible without the assistance of DIMES (Delft Institute of Microsystems and Nanoelectronics). This work is supported in part by project BSIC, Misat IC2.

References

[1] Gad-el-Mak M 1999 The fluid mechanics of microdevices *J. Fluids Eng. ASME* **121** 5–33
[2] Bao M and Yang H 2007 Squeeze film air damping in MEMS *Sensors Actuators* A **136** 3–27
[3] Darling R B, Hivick C and Xu J 1998 Compact analytical modeling of squeeze film damping with arbitrary venting conditions using a Green's function approach *Sensors Actuators* A **70** 32–41
[4] Sumali H 2007 Squeeze-film damping in the free molecular regime: model validation and measurement on a MEMS *J. Micromech. Microeng.* **17** 2231–40
[5] Knudsen M 1934 *The Kinetic Theory of Gases* (London: Methuen)
[6] Langlois W E 1962 *Q. Appl. Math.* **20** 131–50
[7] Blech J J 1983 On isothermal squeeze films *J. Lubr. Technol.* **105** 615–20
[8] Christian R G 1966 The theory of oscillating-vane vacuum gauges *Vacuum* **16** 175
[9] Newel W E 1967 Miniaturization of tuning forks *Science* **161** 1320–6
[10] Kadar Z, Kindt W, Bossche A and Mollinger J 1996 Quality factor of torsional resonators in the low-pressure region *Sensors Actuators* A **53** 299–303

[11] Li B, Wu H, Zhu C and Lui J 1999 The theoretical analysis on damping characteristics of resonant microbeam in vacuum *Sensors Actuators* A **77** 191–4
[12] Bao M, Yang H, Yin H and Sun Y 2002 Energy transfer model for squeeze-film air damping in low vacuum *J. Micromech. Microeng.* **12** 341–6
[13] Veijola T 2004 Compact models for squeezed-film dampers with inertial and rarefied gas effects *J. Micromech. Microeng.* **14** 1109–18
[14] Hutcherson S and Ye W 2004 On the squeeze-film damping of micro-resonators in the free-molecule regime *J. Micromech. Microeng.* **14** 1726–33
[15] Schaaf S A and Chambre P L 1961 *Flow of Rarefied Gases* (Princeton, NJ: Princeton University Press)
[16] Miller K, Cowen A, Hames G and Hardy B 2004 *SOIMUMPs Design Handbook* from http://www.memsrus.com/documents/SOIMUMPs.dr.v4.pdf